

**This is a self-archived version of an original article. This version may differ from the original in pagination and typographic details.**

**Author(s):** Lhersonneau, Gérard; Wöhr, A.; Pfeiffer, B.; Kratz, K.-L.; Collaboration, ISOLDE

**Title:** First decay study of the very neutron-rich isotope  $^{93}\text{Br}$

**Year:** 2001

**Version:** Accepted version (Final draft)

**Copyright:** © 2001, American Physical Society

**Rights:** In Copyright

**Rights url:** <http://rightsstatements.org/page/InC/1.0/?language=en>

**Please cite the original version:**

Lhersonneau, Gérard, Wöhr, A., Pfeiffer, B., Kratz, K.-L., Collaboration, ISOLDE. (2001). First decay study of the very neutron-rich isotope  $^{93}\text{Br}$ . *Physical Review C*, 63(3), Article 034316. <https://doi.org/10.1103/PhysRevC.63.034316>

# First decay study of the very neutron-rich isotope $^{93}\text{Br}$

G. Lhersonneau,<sup>1,2</sup> A. Wöhr,<sup>1,3</sup> B. Pfeiffer,<sup>1</sup> K.-L. Kratz,<sup>1</sup>  
and the ISOLDE Collaboration<sup>4</sup>

<sup>1</sup>*Institut für Kernchemie, Universität Mainz, D-55099 Mainz, Germany*

<sup>2</sup>*Department of Physics, University of Jyväskylä, P.O. Box 35, FIN-40351 Jyväskylä, Finland*

<sup>3</sup>*Clarendon Laboratory, University of Oxford, Oxford OX1 3PU, United Kingdom*

<sup>4</sup>*CERN, CH-1211 Geneva 23, Switzerland*

(Received 3 November 2000; published 20 February 2001)

The decay of the mass-separated, very neutron-rich isotope  $^{93}\text{Br}$  has been studied by  $\gamma$  spectroscopy. A level scheme of its daughter  $^{93}\text{Kr}$  has been constructed. Level energies,  $\gamma$ -ray branching ratios, and multipolarities suggest spins and parities which are in accord with a smooth systematics of the  $N=57$  isotones for  $Z\leq 40$ , suggesting the  $N=56$  subshell closure still to be effective in Kr isotopes. So far, there is no indication of a progressive onset of deformation in neutron-rich Kr isotopes.

DOI: 10.1103/PhysRevC.63.034316

PACS number(s): 27.60.+j, 23.20.Lv

## I. INTRODUCTION

Neutron-rich krypton isotopes are located in an interesting mass region where competition of various structures and shapes at low-excitation energy occurs. With  $Z=36$ , the Kr isotopes lie roughly in the middle between the classical proton shell closures at  $Z=28$  and  $50$ . It is therefore expected that the addition of only a few neutrons to the  $N=50$  shell, would soon lead to the development of collective features. On the one hand, this situation, indeed, corresponds to the  $Z=42$  molybdenum isotopes which are located symmetrically to krypton with respect to the proton midshell at  $Z=39$ . On the other hand, however, this picture is at variance with the systematics established for the immediate  $Z>36$  neighbor isotopes of Kr. Especially, the even-even nuclei of strontium and zirconium experience a strong closure of the  $d_{5/2}$  neutron subshell at  $N=56$ . The  $2^+$  states in  $^{96}\text{Zr}$  and  $^{98}\text{Zr}$  are quite high with a maximum energy of 1751 keV for  $^{96}\text{Zr}$  [1,2]. The  $2^+$  states of Sr, although lower than in their Zr isotones, are with about 800 keV still fairly high in this region and exhibit little collectivity [3]. Nevertheless, a deformed minimum in the potential energy surface at about 1.5 MeV has been reported for the  $N=58$  isotones  $^{96}\text{Sr}$  and  $^{98}\text{Zr}$ , based on very large  $\rho^2(E0)$  values [4] and rotational band structures [5]. These deformed structures rapidly come down in energy with increasing neutron number, until the  $N=60$  isotones  $^{98}\text{Sr}$  and  $^{100}\text{Zr}$  exhibit well developed rotational ground-state bands [5]. Yet,  $0^+$  states at very low energies, at 215 and 331 keV, respectively, have been interpreted as signatures of shape coexistence [6]. A similar shape transition is also observed in  $Z=39$  yttrium isotopes [7–9]. So far, the heaviest  $Z=37$  rubidium isotope studied by  $\gamma$ -spectroscopy is  $^{94}\text{Rb}$ , with  $N=57$  the nearest neighbor isotone of  $^{93}\text{Kr}$ . Its low-lying levels were interpreted in the interacting boson-fermion-fermion frame as being spherical [10]. Published information on levels in Kr isotopes heavier than  $^{90}\text{Kr}$  remained rather scarce until recently. It consisted only of  $\beta$ -decay studies leading to levels in  $^{91-93}\text{Kr}$  performed by some of us presented in preliminary reports [11–14] and in a Ph.D. thesis [15]. However, near completion of

this manuscript we became aware of a prompt-fission study of the even-even  $^{88-94}\text{Kr}$  [16]. The data do not show evidence for an increasing softness towards deformation, at least until the  $N=58$   $^{94}\text{Kr}$  nucleus.

In addition to  $\gamma$  spectroscopy, laser spectroscopic experiments have been carried out in this region. The sudden increase of the square charge radius  $\langle r^2 \rangle$  at  $N=60$  in the Rb and Sr isotopic chains was interpreted as due to the onset of strong ground-state deformation [17–19]. In contrast, more recent laser spectroscopic measurements on Kr isotopes up to  $N=60$ , did not reveal such a significant increase in the  $\langle r^2 \rangle$  values [20]. Hence, the onset of ground-state deformation in the Kr isotopes either seems to be delayed to larger neutron numbers, or will occur more gradually than in the immediate  $Z$  neighbors. Detailed spectroscopic studies should be able to answer these questions either in showing the existence of deformed excited states coexisting with spherical states of similar character as those in the Sr and Zr isotopes, or in showing a smooth change from spherical to transitional structures as in the Mo isotopes when approaching  $N=60$ .

For these reasons, spectroscopic investigations of the decays of neutron-rich bromine isotopes to their krypton daughter nuclei would be of great interest. However, even today the separation of short-lived halogen isotopes by negative surface ionization remains an experimental challenge to ion-source technology. As one of the last experiments at the old ISOLDE on-line mass separator at CERN before the shut-down of the SC, neutron-rich Kr isotopes around  $N=56$  were studied for the first time and so far only by  $\gamma$ - and delayed-neutron spectroscopy [15]. Here, we report on the decay of  $N=58$   $^{93}\text{Br}$  to  $^{93}\text{Kr}$ , the most neutron-rich isotope of this element so far observed by radioactivity.

## II. EXPERIMENT

The  $\beta$ -decay parent nucleus  $^{93}\text{Br}$  was produced by 600 MeV proton-induced fission of uranium. A beam of negatively charged bromine ions was obtained by a chemically selective  $\text{LaB}_6$  surface ion source [21], and was collected at the detection position on a moving tape system. The  $\gamma$  rays following  $\beta$  decay of  $^{93}\text{Br}$  were measured with various detectors: two coaxial Ge detectors for transitions up to about 4

TABLE I. List of transitions assigned to the decay of  $^{93}\text{Br}$  to  $^{93}\text{Kr}$ . Taking into account the intensity of unplaced transitions, 100  $\gamma$ -intensity units correspond to 60% branching in this decay mode, i.e., a 19% decay branch for  $^{93}\text{Br}$  ( $P_n = 68\%$ ).

Energy (keV)	Intensity (%)	Placed		Coincidences
		from	to	
117.4 (2)	100.0 (50) <sup>a</sup>	117	0	237, 242, 446, 593, 670, (1220) <sup>c</sup>
237.4 (2)	29.6 (25) <sup>a</sup>	355	117	117, (629) <sup>c</sup>
242.0 (2)	59.8 (7.5) <sup>a</sup>	359	117	117, 350, 446, 670, 966, 978, 1142 <sup>c</sup>
349.9 (5)	3.6 (21) <sup>b</sup>	710	359	
359.4 (2)	3.7 (7) <sup>a</sup>	359	0	
446.0 (2)	6.8 (9) <sup>a</sup>	805	359	117, 242
592.7 (4)	10.6 (26) <sup>b</sup>	710	117	117
669.5 (3)	3.4 (5) <sup>a</sup>	1029	359	(117, 242)
687.9 (2)	5.3 (4) <sup>a</sup>	805	117	(117)
710.2 (2)	19.7 (18) <sup>a</sup>	710	0	
966.4 (7)	5.9 (39) <sup>b</sup>	1326	359	(117, 242)
977.6 (6)	6.5 (43) <sup>b</sup>	1337	359	(117, 242)
2103.5 (4)	19.4 (27) <sup>a</sup>			d
2224.7 (4)	4.3 (12) <sup>a</sup>			d
3085.8 (7)	1.4 (4) <sup>a</sup>			d
3606.3 (6)	7.8 (10) <sup>a</sup>			d

<sup>a</sup>Intensity from singles spectra.

<sup>b</sup>Intensity from coincidence data only.

<sup>c</sup>Unplaced weak transition with  $\delta E_\gamma \approx 1$  keV and  $I_\gamma \leq 1$ .

<sup>d</sup>Unplaced transition assumed a g.s. transition for calculation of  $\beta$  feedings.

MeV, a small planar Ge detector for low energies and a  $\text{BaF}_2$  scintillator. In addition, a thin plastic scintillator was used to detect  $\beta$  particles.

The low threshold of 8 keV of the planar detector allowed the measurement of Kr  $K$  x rays necessary for  $Z$  identification as well as for the application of the fluorescence method. In this method,  $K$ -conversion coefficients are measured by the intensity ratio of the  $K$  x-ray peak to the one of the photopeak of the converted transition. In order to ensure enough selectivity, the method must be applied to spectra obtained by gating selected transitions. The coincidence efficiency was determined by using a  $^{152}\text{Eu}$  standard source and on-line decay products including Kr, Rb, and Sr activities in the mass chains  $A=91$  to  $93$ . Of particular interest was the 142.4 keV line in  $^{92}\text{Rb}$  which has  $M1$  multipolarity [2]. The low statistics for the  $A=93$  mass chain limited the use of the most accurate timing methods based on coincidences between the planar Ge detector, the plastic-scintillator and the  $\text{BaF}_2$  crystal. Yet, delayed  $\gamma$ - $\gamma$ - $t$  coincidences recorded with the large Ge detectors allowed observation of level lifetimes typically longer than 10 ns.

A valid coincidence event was defined by hardware to include at least one of the signals from the planar detector or one of the coaxial Ge detectors. Coincidence events were recorded in list mode with the GOOSY system at ISOLDE. They were off-line sorted on a VAX computer to create subsets of energy-energy-time triplets for subsequent gating and generation of energy or time projections.

### III. RESULTS

The identification of the new  $\gamma$  lines following the decay of  $^{93}\text{Br}$  was made on the basis of the coincidence relations

and the additional requirement that the characteristic x rays of Kr had to be present in the coincidence spectra. In addition to  $^{93}\text{Br}$  and its decay products, a contamination of the  $A=93$  beam due to  $[\text{}^{83}\text{Se}^{10}\text{B}]^-$  molecular ions was observed. This contamination could be identified unambiguously by comparing the intensities of  $\gamma$  lines in singles spectra recorded at  $A=93$  and  $A=94$ . In these spectra, the intensities of the contaminant  $^{83}\text{Se}$  lines varied according to the abundance ratio of  $^{11}\text{B}/^{10}\text{B}$ . The  $Z$  selectivity of the negative ion source for bromine was verified by comparing the  $\beta$ -delayed neutron emission probability,  $P_n$ , of  $^{91}\text{Br}$  from  $\gamma$ -spectroscopic data obtained during this experiment with earlier  $\beta n$ -multiscaling measurements [22]. The  $\gamma$ -spectroscopic method is based on comparison of activities in the  $A=90$  and  $A=91$  chains. The result,  $P_n = 36(2)\%$ , was found to be in reasonable agreement with the value  $30(2)\%$  of Ref. [22], thus indicating that there was no sizeable negative ionization of  $A=91$  isobars apart from  $^{91}\text{Br}$ . Consequently, it was justified to determine also the  $P_n$  value of  $^{93}\text{Br}$  by comparing known  $\gamma$  intensities of the decays of the  $A=93$  daughter isotopes  $^{93}\text{Kr}$ ,  $^{93}\text{Rb}$ , and  $^{93}\text{Sr}$  with those from  $A=92$  isobars, in particular  $^{92}\text{Rb}$ . In this way, we obtain a rather large value of  $P_n = 68(7)\%$  for  $^{93}\text{Br}$  decay. The transitions in  $^{93}\text{Kr}$  populated by  $^{93}\text{Br}$  decay are listed in Table I and the decay scheme is shown in Fig. 1.

The spin and parity of  $^{93}_{35}\text{Br}$  are not known experimentally. In the  $_{37}\text{Rb}$  isotopes ground-state spins vary between  $I = 3/2$  and  $5/2$ . The spherical shell model predicts odd parity, associated with the  $p_{3/2}$  and  $f_{5/2}$  orbitals, respectively. Both alternatives remain for  $^{93}\text{Br}$ .

According to level systematics of the  $N=57$  isotones, the ground state of  $^{93}\text{Kr}$  should have  $I^\pi = 1/2^+$ . This spin was

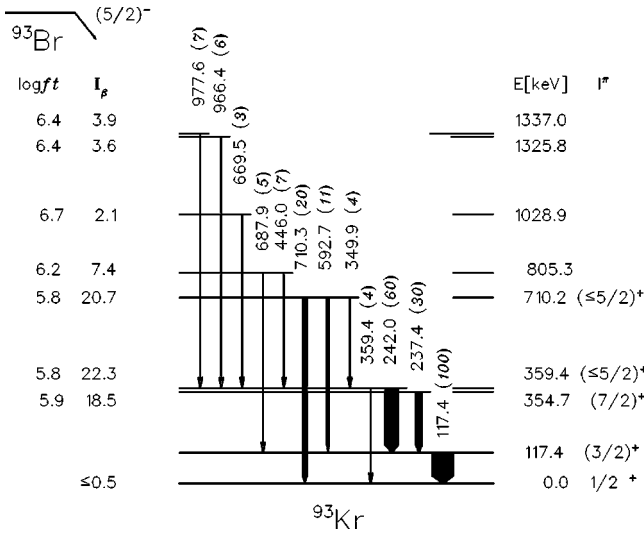


FIG. 1. Partial decay scheme of  $^{93}\text{Br}$  to  $^{93}\text{Kr}$ . In calculating the  $\beta$  feedings it has been taken into account that a fraction of the observed  $\gamma$ -ray intensity is not placed in the scheme; see Table I.

deduced for  $^{93}\text{Kr}$  and  $^{95}\text{Sr}$  from laser spectroscopy [18,20] and  $I^\pi=1/2^+$  was determined from transfer reactions for  $^{97}\text{Zr}$  [23]. These spin and parity correspond to the  $\nu s_{1/2}$  orbital. In the present experiment, the ground-state feeding has been deduced from a comparison of  $\gamma$ -ray intensities of transitions assigned to  $^{93}\text{Kr}$  and to its daughters  $^{93}\text{Rb}$  and  $^{93}\text{Sr}$ . As for the  $P_n$  estimate, this method relies on the assumption that the negative-ion source was selective for bromine. With this approach, no sizable  $\beta$  branch was found to the ground state of  $^{93}\text{Kr}$ . This result is consistent with the assumed change of parity, but yet does not preclude positive parity of  $^{93}\text{Br}$  if  $I > 3/2$ .

The level at 117.4 keV is the first excited state in  $^{93}\text{Kr}$ . It is based on the fact that the  $\gamma$  line of this energy clearly is the strongest one assigned to  $^{93}\text{Br}$  decay. A conversion coefficient  $\alpha_K=0.058(10)$  is measured which implies a dipole transition [ $\alpha_K(E1)=0.050, \alpha_K(M1)=0.075, \alpha_K(E2)=0.43$ ]. Shell-model considerations, which exclude a parity change among low-spin levels, lead to the  $M1$  assignment and  $I^\pi=(1/2, 3/2)^+$ .

The next levels at 354.8 and 359.4 keV are based on the strong  $\gamma$  lines at 237.4 and 242.0 keV seen in coincidence with the 117.4 keV ground-state transition. The latter level is further supported by the observation of a weak 359.4 keV crossover transition to the ground state. The conversion coefficients for the above 237.4 and 242.0 keV lines cannot be measured independently of each other. In the 117 keV gate, both lines contribute to the  $K$  x-ray peak. The intensity indicates, however, that one of the transitions is predominantly of  $M1$  and the other one of  $E2$  multipolarity. Lifetime measurements indicate that the 237.4 keV line is delayed with respect to the 242.0 keV line; see Fig. 2. Since the feedings of the 354.8 keV and 359.4 keV levels by  $\gamma$ -rays are weak, a wide gate has been used on one of the channels to include the Compton background of unresolved high-energy transitions. The threshold was set to 250 keV to avoid triggering by the lowest-energy events yielding to a too poor timing

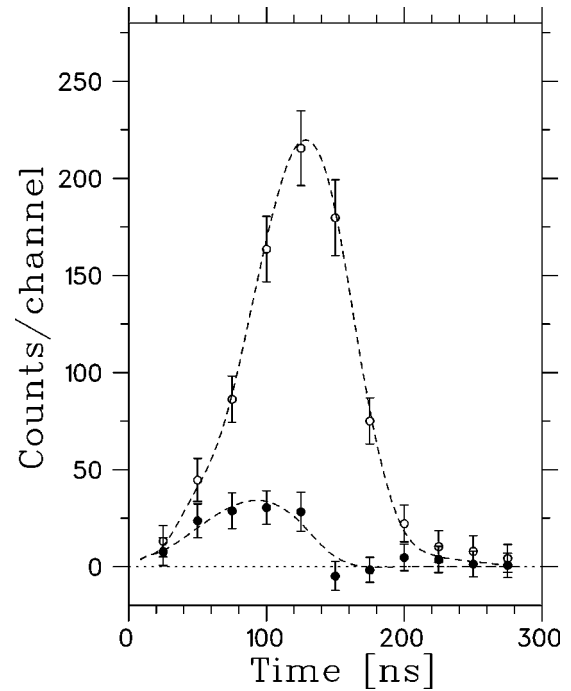


FIG. 2. Time spectra from  $\gamma$ - $\gamma$ - $t$  delayed coincidences. The start signal was given by the selected transitions of 237.4 keV (closed circles) and 242.0 keV (open circles). The stop signal was triggered by the Compton background and photopeaks of any coincident transitions of energy above 250 keV. The physical time axis is from the right to the left. The dashed lines are only a guide to the eye. The absence of a prompt component in the time spectrum of the 237.4 keV transition assigns the delay to originate from the 354.7 keV level and not from another level higher in the scheme.

response. The shift corresponds to a 22(12) ns half-life for the 354.8 keV level. The nondelayed 242.0 keV transition is unlikely  $E2$  but the  $M1$ . Consequently, the 237.4 keV transition is a slightly enhanced  $E2$ , the Weisskopf unit being 29 ns. Based on these results, the 117.4 keV level could have a spin and parity of  $3/2^+$ , the 354.8 keV level  $I^\pi=7/2^+$ , and the 359.4 keV level  $I^\pi=(1/2, 3/2, 5/2)^+$ . These spins provide a simple explanation for the existence of a crossover transition from the 359.4 keV level to the ground state but not from the 354.8 keV level. Further levels are placed according to their coincidence relationships and energy sum fitting. The highest of the relatively strongly fed levels at 710.2 keV has a maximum spin of  $5/2^+$ . However, the sizable ground-state branching rather favors  $(1/2, 3/2)^+$ .

The vanishing  $\beta$  branch to the  $1/2^+$  ground state of  $^{93}\text{Kr}$  and the relatively strong feedings of the 354.8 keV (proposed as  $7/2^+$ ) and 359.4 keV levels can be interpreted in a consistent manner if a spin and parity of  $I^\pi=5/2^-$  is assumed for  $^{93}\text{Br}$ . In this case, a further consequence of the  $\beta$  feeding of the 359.4 and 710.2 keV levels is that they cannot be  $1/2^+$  states. We note that the  $\log ft$  values to these levels must be regarded as lower limits due to the non-neglectable probability that many weak  $\beta$  branches to levels between 1.35 MeV and the neutron separation energy of  $S_n \approx 3.4$  MeV have remained unobserved. In any case, these  $\log ft$  limits are in

TABLE II. Levels in  $^{93}\text{Kr}$  fed in  $\beta$  decay of  $^{93}\text{Br}$ .  $\log ft$  values are calculated with  $T_{1/2}(^{93}\text{Kr}) = 102$  ms [11],  $Q_\beta = 11.02$  MeV [35], and  $P_n = 68\%$  (this work). The  $\beta$  feedings are for 100 decays to  $^{93}\text{Kr}$ , i.e., a 32% decay branch of  $^{93}\text{Br}$ . Unplaced high-energy transitions account for a total of about 20%  $\beta$  feeding not listed here.

Energy (keV)	$\beta$ feeding %	$\log ft$	$I^\pi$
0	$\leq 0.5$	$> 7.5$	$1/2^+$
117.4 (2)	1.3 (58)		$(3/2)^+$
354.7 (3)	18.5 (22)	5.9	$(7/2)^+$
359.4 (2)	22.3 (50)	5.8	$(3/2, 5/2)^{+a}$
710.2 (2)	20.7 (35)	5.8	$(5/2, 3/2)^{+a}$
805.3 (2)	7.4 (9)	6.2	
1028.9 (4)	2.1 (4)	6.7	
1325.8 (7)	3.6 (23)	6.4	
1337.0 (6)	3.9 (25)	6.4	

<sup>a</sup>First value is preferred on basis of systematics.

agreement with general expectations for first-forbidden transitions. Level properties are shown in Table II.

#### IV. DISCUSSION

In order to understand the above results for  $^{93}\text{Kr}$ , it is worthwhile to compare them to existing data for neighboring  $N=57$  isotones. It is quite obvious that a dramatic discontinuity in the  $N=57$  systematics occurs at  $^{97}\text{Zr}$ , i.e., at  $Z=40$  when protons start to occupy the  $g_{9/2}$  subshell [24]. The level structures of  $Z \geq 42$  nuclei do not show signatures of the  $N=56$  gap associated with the spherical  $\nu d_{5/2}$  subshell closure. In this region, the  $d_{5/2}$  and  $g_{7/2}$  neutron orbitals are remarkably close to each other. Furthermore, the  $\nu s_{1/2}$  level comes down rapidly in energy when protons are removed and becomes the ground state in  $^{99}_{42}\text{Mo}$ . When reaching  $^{97}_{40}\text{Zr}$

and continuing towards even lower  $Z$  values, the first excited state is a  $3/2^+$  level while the  $d_{5/2}$  orbital has not been identified but is not any longer a quasiparticle below  $g_{7/2}$  [25,26]. Calculations performed for the  $N=59$  isotones  $^{97}\text{Sr}$  and  $^{99}\text{Zr}$ , where a similar level structure exists, indicate a rather complex character of this  $3/2^+$  level, thus excluding the  $d_{3/2}$  single neutron parentage [27,28]. Its structure rather consists mainly of  $g_{7/2}$  and  $d_{3/2}$  neutron components coupled to core states. The results from the above theoretical work may also probably be applied to the present work on  $^{93}\text{Kr}$ . Accordingly, we propose that the 117.4 keV level represents this complex  $3/2^+$  state, and that the 354.8 keV level is the  $\nu g_{7/2}$  orbital.

We tentatively propose assignments for some higher-lying levels using systematics of energies and branching ratios for  $N=57$  and  $59$  isotones. These levels are shown in Fig. 3. The next strongly fed levels, at 359 and 710 keV, could be the second  $3/2^+$  and  $5/2^+$  doublet based on the  $2 \otimes s_{1/2}$  core-plus-particle coupling. According to the IBFM calculations for  $^{97}\text{Sr}$  [27], the 523 keV level is the  $3/2_2^+$  state. Its characteristic feature is a large branching ratio for the  $3/2_2^+ \rightarrow 3/2_1^+$  transition. By analogy, the 355 keV level in  $^{93}\text{Kr}$  and the 1012 keV level in  $^{95}\text{Sr}$  could be the  $3/2_2^+$  states in these nuclei. In  $^{97}\text{Sr}$  the  $5/2_1^+$  level at 600 keV has an  $E2$  transition to the ground state which is several times stronger than the  $M1$  to the  $3/2_1^+$  level. The 710 keV level in  $^{93}\text{Kr}$  has similar branching ratios. In  $^{95}\text{Sr}$ , there are two possible  $5/2^+$  levels at 681 and 1004 keV [25]. Both  $\beta$ -decay parents of  $^{93}\text{Kr}$  and  $^{95}\text{Sr}$  are  $5/2^-$  states. Thus  $\log ft$  values could be used to tentatively favor the 681 keV level ( $\log ft=6.0$ ) over the 1004 keV level ( $\log ft=6.8$ ) as being the partner level of the 710 keV level in  $^{93}\text{Kr}$  ( $\log ft=5.8$ ).

From the similarities of the low-lying levels of the  $N=57$  isotones of krypton and strontium (see Fig. 3) we conclude that for  $^{93}\text{Kr}$ , as in its neighbor  $^{95}\text{Sr}$ , there is so far no

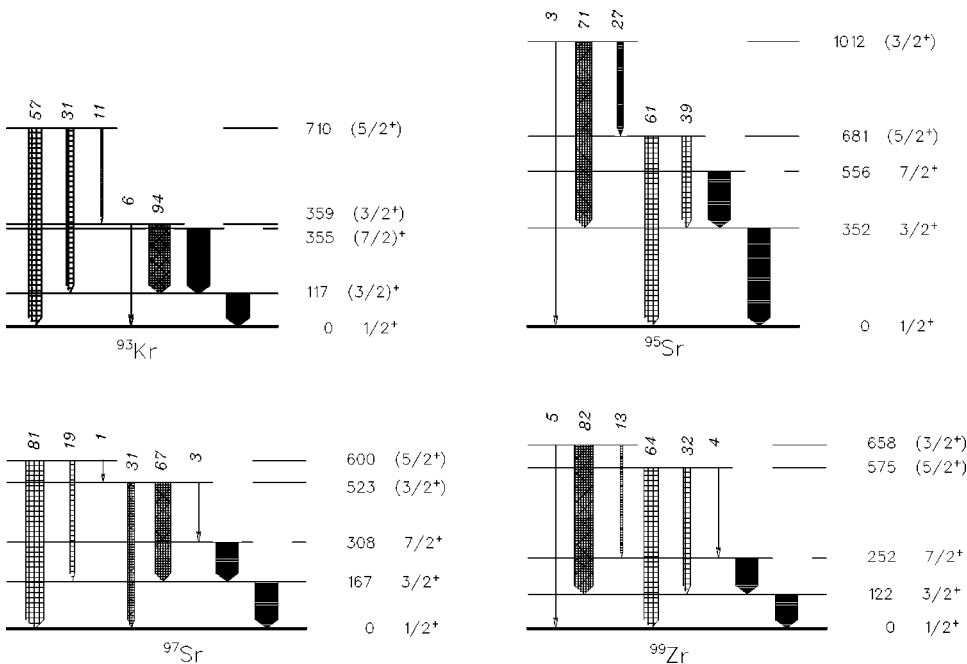


FIG. 3. The lowest-lying levels in the  $N=57$  isotones  $^{93}\text{Kr}$ ,  $^{95}\text{Sr}$  (top) and the  $N=59$  isotones  $^{97}\text{Sr}$  and  $^{99}\text{Zr}$  (bottom). The similarities suggest the survival of the  $N=56$  subshell closure in Kr isotopes, in contrast to the more transitional character of Mo isotopes located symmetrically with respect to the  $Z=39$  midshell.

signature of increased collectivity at low excitation energy. This was already indicated by the rather high energy of  $2^+$  states in even-even isotopes, 769 keV for  $^{92}\text{Kr}_{56}$  [11,12] and 665 keV for  $^{94}\text{Kr}_{58}$  [14–16]. These energies are somewhat lower than in their strontium isotones, e.g., 815 keV for  $^{96}\text{Sr}_{58}$ , but remain higher than in molybdenum isotopes, e.g., 536 keV in  $^{100}\text{Mo}_{58}$ . We note that a similar  $1/2^+$ ,  $3/2^+$ , and  $7/2^+$  level sequence is exhibited by  $^{97}\text{Zr}$ , with however, much larger level spacings due to the immediate neighborhood of  $^{96}\text{Zr}$  where the  $Z=40$  and  $N=56$  subshell closures reinforce each other [26]. In contrast, the levels in  $^{99}\text{Mo}$  exhibit a different order, with a  $5/2^+$  first excited state associated to the  $d_{5/2}$  neutron instead of the  $3/2^+$  complex level [24]. The close similarity of Kr isotopes ( $Z=36$ ) with their Sr isotones ( $Z=38$ ) but the differences with Mo ( $Z=42$ ) indicates that there is no symmetry with respect to the  $Z=39$  proton midshell. This is in contrast to the simple picture of describing nuclear structure in terms of the number of valence particles or holes only.

One may, however, speculate that—as observed in the  $N=57$ – $59$  Sr and Zr isotopes [25,27,28]—also their respective Kr isotones will exhibit coexistence of spherical states at low energy and levels of deformed collective nature at higher energy. Spherical-to-deformed shape transitions between  $N=58$  and  $N=60$  were already predicted as early as 1981 by Bucurescu *et al.* [29] who had calculated potential-energy surfaces in a microscopic-macroscopic approach. Also Möller *et al.* had predicted shape coexistence in this mass region within their 1981 finite-range droplet model (FRDM) [30,31], however not between spherical and deformed states but rather between prolate and oblate shapes. More recently, similar features were predicted in relativistic mean-field (RMF) calculations by Lalazissis *et al.* [32] in an attempt to reproduce the laser-spectroscopic measurements of the mean squared charge radii  $\langle r^2 \rangle$  of neutron-rich Sr and Kr isotopes [17–19].

The  $P_n$  value of  $^{93}\text{Br}$  decay is 68(7)%. This large delayed-neutron branch and, in consequence, the weak  $\beta$  feeding to low-lying states in  $^{93}\text{Kr}$  can easily be understood in terms of general nuclear-structure signatures in this mass region. Spherical shell-model calculations of Gamow-Teller (GT) decay of  $^{93}\text{Br}$  using the quasi-particle random-phase approximation (QRPA) with a folded-Yukawa single-particle potential and a Lipkin-Nogami pairing model [33]

predict the lowest allowed  $\beta$  transitions at 5.2 MeV and 6.0 MeV in  $^{93}\text{Kr}$ , respectively, well above the neutron-separation energy of  $S_n \approx 3.4$  MeV [34,35]. These are the  $\nu g_{7/2} \rightarrow \pi g_{9/2}$  3QP and the  $\nu p_{3/2} \rightarrow \pi p_{1/2}$  1QP transition, respectively. Hence, the low-energy part of the  $^{93}\text{Kr}$  spectrum is only fed by relatively weak first-forbidden (ff)  $\beta$  transitions. When taking into account the ff-strength distribution according to the Gross theory [36], our calculations yield a delayed-neutron emission branch of  $P_n = 83\%$ , in fair agreement with the experimental observation. It is interesting to note in this context, that QRPA calculations using the deformation parameters of  $\epsilon \approx 0.25$  as predicted, e.g., by the global mass models FRDM and ETFSI-1 [34,37] already shift some GT strength below  $S_n$  in  $^{93}\text{Kr}$ , thus resulting in a  $P_n$  value of only about 25%, in disagreement with experiment.

## V. CONCLUSION

The decay of  $N=58$   $^{93}\text{Br}$  has been studied for the first time and a partial decay scheme of  $^{93}\text{Kr}$  has been constructed. The low-lying states extend the level systematics of the  $N=57$  isotones. The good correspondence with the levels in  $^{95}\text{Sr}$  suggests that the spherical  $N=56$  shell gap is still effective for the  $Z=36$  Kr isotopes. So far, no signatures of an increase of collectivity leading to a transitional character have been observed. Shape coexistence in Kr isotopes is likely to occur for  $N \geq 58$  with features similar to those well established in the Sr and Zr isotones. The fact that—according to laser spectroscopic measurements—the onset of ground-state deformation does not occur at  $N=60$ , may imply that the postulated deformed levels in the Kr isotopes lie higher and/or decrease slower in energy than in the corresponding Sr and Zr isotones. Hence, it would be of great interest to search for fingerprints of deformation in even heavier Kr isotopes, although still today this represents a real experimental challenge.

## ACKNOWLEDGMENTS

This work was performed under support of the German BMFT and has been completed under support of the Finnish Centre of Excellence Programme 2000–2005 (Project No. 44875, Nuclear and Condensed Matter Physics Programme). The authors wish to thank Dr. W. Urban for communicating a manuscript prior to publication.

- 
- [1] L. K. Peker, Nucl. Data Sheets **68**, 165 (1993).  
 [2] R. B. Firestone and V. S. Shirley, *Table of Isotopes*, 8th ed. (Wiley, New York, 1996).  
 [3] H. Mach, F. K. Wohn, G. Molnar, K. Sistemich, J. C. Hill, M. Moszynski, R. L. Gill, W. Krips, and D. S. Brenner, Nucl. Phys. **A523**, 197 (1991).  
 [4] G. Lhersonneau, B. Pfeiffer, K.-L. Kratz, T. Enqvist, P. P. Jauho, A. Jokinen, J. Kantele, M. Leino, J. M. Parmonen, H. Penttilä, J. Äystö, and the ISOLDE Collaboration, Phys. Rev. C **49**, 1379 (1994).  
 [5] J. H. Hamilton, A. V. Ramayya, S. J. Zhu, G. M. Ter-Akopian, Yu. Oganessian, J. D. Cole, J. O. Rasmussen, and M. A. Stoyer, Prog. Part. Nucl. Phys. **35**, 635 (1995).  
 [6] H. Mach, F. K. Wohn, M. Moszynski, R. L. Gill, and R. F. Casten, Phys. Rev. C **41**, 1141 (1990).  
 [7] G. Lhersonneau, S. Brant, V. Paar, and D. Vretenar, Phys. Rev. C **57**, 681 (1998).  
 [8] G. Lhersonneau, R. A. Meyer, K. Sistemich, H. P. Kohl, H. Lawin, G. Menzen, H. Ohm, T. Seo, and H. Weiler, in *Nuclei Off the Line of Stability*, 190th Meeting of the ACS, Chicago,

- 1985, edited by R. A. Meyer and D. S. Brenner, ACS Symposium Series 324 (American Chemical Society, Washington, 1986), p. 202.
- [9] R. A. Meyer, E. Monnard, J. A. Pinston, F. Schussler, B. Pfeiffer, and V. Paar, *Z. Phys. A* **327**, 393 (1987).
- [10] G. Lhersonneau, S. Brant, H. Ohm, V. Paar, K. Sistemich, and D. Weiler, *Z. Phys. A* **334**, 259 (1989).
- [11] K.-L. Kratz, H. Gabelmann, B. Pfeiffer, P. Möller, and the ISOLDE Collaboration, *Z. Phys. A* **330**, 229 (1988).
- [12] B. Pfeiffer, K.-L. Kratz, H. Gabelmann, and P. Möller, Annual Report, 1988, Institut für Kernchemie, Mainz, IKMz 89-1, 14, 1989, ISSN 0932-7622.
- [13] A. Wöhr, H. Gabelmann, K.-L. Kratz, G. Lhersonneau, V. Paar, B. Pfeiffer, F. Schäfer, H. Sohn, and the ISOLDE Collaboration, Annual Report, 1989, Institut für Kernchemie, Mainz, IKMz 90-1, 10, 1990, ISSN 0932-7622.
- [14] A. Wöhr, H. Gabelmann, G. Lhersonneau, B. Pfeiffer, K.-L. Kratz, and the ISOLDE Collaboration, in *Proceedings of the 6th International Conference on Nuclei far from Stability and 9th International Conference on Atomic Masses and Fundamental Constants*, Bernkastel-Kues, Germany, 1992, edited by R. Neugart and A. Wöhr, Inst. Phys. Conf. Ser. No. 132 (IOP, Bristol, 1993), p. 867.
- [15] A. Wöhr, Ph.D. thesis, Universität Mainz, 1992.
- [16] T. Rząca-Urban, W. Urban, A. Kaczor, J. L. Durell, M. J. Leddy, M. A. Jones, W. R. Phillips, A. G. Smith, B. J. Varley, I. Ahmad, L. R. Morss, M. Bentaleb, E. Lubkiewicz, and N. Schulz, *Eur. Phys. J. A* **9**, 165 (2001).
- [17] C. Thibault, *Hyperfine Interact.* **24**, 95 (1985).
- [18] R. E. Silverans, P. Lievens, L. Vermeeren, E. Arnold, W. Neu, R. Neugart, K. Wendt, F. Buchinger, E. B. Ramsay, and G. Ulm, *Phys. Rev. Lett.* **60**, 2607 (1988).
- [19] P. Lievens, R. E. Silverans, L. Vermeeren, W. Borchers, W. Neu, R. Neugart, K. Wendt, F. Buchinger, E. Arnold, and the ISOLDE Collaboration, *Phys. Lett. B* **256**, 141 (1991).
- [20] M. Keim, E. Arnold, W. Borchers, U. Georg, A. Klein, R. Neugart, L. Vermeeren, R. E. Silverans, and P. Lievens, *Nucl. Phys. A* **586**, 219 (1995).
- [21] B. Vosicki, T. Björnstad, L. C. Carraz, J. Heinemeier, and H. L. Ravn, *Nucl. Instrum. Methods Phys. Res.* **186**, 307 (1981).
- [22] G. T. Ewan, P. Hoff, B. Jonson, K.-L. Kratz, P. O. Larsson, G. Nyman, H. L. Ravn, and W. Ziegert, *Z. Phys. A* **318**, 309 (1984).
- [23] A. Artna-Cohen, *Nucl. Data Sheets* **70**, 85 (1993).
- [24] G. Lhersonneau, B. Pfeiffer, J. R. Persson, J. Suhonen, J. Toivanen, P. Campbell, P. Dendooven, A. Honkanen, M. Huhta, P. M. Jones, R. Julin, S. Juutinen, M. Oinonen, H. Penttilä, K. Peräjärvi, A. Savelius, W. Jicheng, J. C. Wang, and J. Äystö, *Z. Phys. A* **358**, 317 (1997).
- [25] K.-L. Kratz, H. Ohm, A. Schröder, H. Gabelmann, W. Ziegert, B. Pfeiffer, G. Jung, E. Monnard, J. A. Pinston, F. Schussler, G. I. Crawford, S. G. Prussin, and Z. M. de Oliveira, *Z. Phys. A* **312**, 43 (1983).
- [26] G. Lhersonneau, P. Dendooven, A. Honkanen, M. Huhta, P. M. Jones, R. Julin, S. Juutinen, M. Oinonen, H. Penttilä, J. R. Persson, K. Peräjärvi, A. Savelius, J. C. Wang, and J. Äystö, *Phys. Rev. C* **56**, 2445 (1997).
- [27] G. Lhersonneau, B. Pfeiffer, K.-L. Kratz, H. Ohm, K. Sistemich, S. Brant, and V. Paar, *Z. Phys. A* **337**, 149 (1990).
- [28] S. Brant, V. Paar, and A. Wolf, *Phys. Rev. C* **58**, 1349 (1998).
- [29] D. Bucurescu, G. Constantinescu, D. Cutoiu, M. Ivascu, and N. V. Zamfir, *J. Phys. G* **7**, L12 (1981).
- [30] P. Möller and J. R. Nix, *At. Data Nucl. Data Tables* **26**, 165 (1981).
- [31] P. Möller (private communication).
- [32] G. A. Lalazissis and M. M. Sharma, *Nucl. Phys. A* **586**, 201 (1995).
- [33] P. Möller and J. Randrup, *Nucl. Phys. A* **514**, 1 (1990).
- [34] P. Möller, J. R. Nix, W. D. Myers, and W. J. Swiatecki, *At. Data Nucl. Data Tables* **59**, 183 (1995).
- [35] G. Audi, O. Bersillon, J. Blachot, and A. H. Wapstra, *Nucl. Phys. A* **624**, 1 (1997).
- [36] K. Takahashi, M. Yamada, and T. Kondoh, *At. Data Nucl. Data Tables* **12**, 101 (1973).
- [37] Y. Aboussir, J. M. Pearson, A. K. Dutta, and F. Tondeur, *At. Data Nucl. Data Tables* **61**, 127 (1995).